
[View Journal Online](#)
[View Article Online](#)

Theoretical study of the adsorption of BMSF-BENZ drug for osteoporosis disease treatment on Al-doped carbon nanotubes (Al-CNT) as a drug delivery vehicle

 Zaid Husham Al-Sawaff ^{1,2,*}, Serap Senturk Dalgic ³ and Fatma Kandemirli ⁴
¹ Department of Material Science and Engineering, Faculty of Engineering and Architecture, Kastamonu University, 37150, Kastamonu, Turkey

² Medical Instrumentation Technology, Technical Engineering College, Northern Technical University, 41002, Mosul, Iraq

zaidalsawaff@ntu.edu.iq (Z.H.A.)

³ Department of Physics, Faculty of Science, Trakya University, 22030, Edirne, Turkey

dserap@yahoo.com (S.S.D.)

⁴ Department of Biomedical Engineering, Faculty of Engineering and Architecture, Kastamonu University, 37150, Kastamonu, Turkey

fkandemirli@yahoo.com (F.K.)

* Corresponding author at: Medical Instrumentation Technology, Technical Engineering College, Northern Technical University, 41002, Mosul, Iraq.
 e-mail: zaidalsawaff@ntu.edu.iq (Z.H. Al-Sawaff).

RESEARCH ARTICLE



doi 10.5155/eurjchem.12.3.314-322.2143

Received: 08 July 2021

Received in revised form: 31 July 2021

Accepted: 07 August 2021

Published online: 30 September 2021

Printed: 30 September 2021

KEYWORDS

 BMSF-BENZ
 Drug adsorption
 Al-CNT nanotube
 Drug delivery system
 Density functional theory
 Thermodynamic properties

ABSTRACT

The adsorption energy of the BMSF-BENZ adsorbed complexes was investigated to understand the non-local dispersion interactions, with many other chemical parameters related to this subject like HOMO and LUMO, energy gap, and the time needed for the BMSF-BENZ to be desorbed from the nanotube (recovery time). Our study reveals that Al-CNT is a promising adsorbent for this drug as E_{ads} of BMSF-BENZ/Al-CNT complexes are -22.09, -38.68, -12.89, -31.01, -27.31, -21.90, and -21.42 kcal/mol in the gas phase on the active atoms of the BMSF BENZ (Br, N₈, N₉, N₅₈, O₃₅, O₄₁, and S), respectively. In addition, the spontaneous and favorable interaction between the BMSF BENZ and all nanoparticles was confirmed by investigating Gibbs free energy and quantum theory of atoms in molecule analysis (QTAIM) so that it can be used as an electrochemical sensor or biosensor. Furthermore, to more visualize the nature of intermolecular bonding and the strength of interaction between the BMSF-BENZ drug molecule and the nanotube, QTAIM has been widely studied in the case of drug delivery purposes. Al-CNT (4,0) can be extended as a drug delivery system and the work function type sensor.

 Cite this: *Eur. J. Chem.* 2021, 12(3), 314-322

 Journal website: www.eurjchem.com

1. Introduction

Osteoporosis is a disease characterized by low bone mass and the microarchitectural deterioration of bone tissue, leading to bone fragility and increased fracture risk [1]. Most of the therapies used for the treatment of osteoporosis inhibit bone resorption and prevent further bone loss. However, as many osteoporosis patients already lost a large amount of bone at their diagnosis, agents need agents to stimulate new bone formation [2].

This approach's drug and enhancements' discovery goal is to identify a CaSR-antagonist, that is, rapidly absorbed (short Tmax) and fairly rapidly eliminated. Based on its overall *in vitro* and physicochemical properties, one of the BMSF-BENZ derivatives ((4-Bromo-7-methoxy-1-(2-methoxyethyl)-5-([3-(methylsulfonyl) phenyl)methyl]-2-[4-(propane-2-yl)phenyl]-1H-1,3-benzothiazole) (Figure 1) was selected because it showed a sharp PTH-release peak and good properties regarding CaSR receptor [3]. With the increasing development of

nanoscience, varieties of nanostructures such as nanosheets, nanotubes, nano-cones, nanocages, or fullerenes have been widely studied as potential candidates in different fields [4-8]. Among them, nanotubes and nanocages are more suitable candidates for drug carriers due to their fewer side effects, hydrophobic characteristics, high sensitivity towards drug molecules, unique surface properties and atomic structures, etc. [9-11].

CNTs are considered effective gas sensors since they have high surface areas. Two mechanisms were proposed to demonstrate the changes in conductance and capacitance for these CNTs, essentially for alternative current (AC) charge transfers between gas molecules and CNTs that change the conductance and quantum capacitance, and the polarization of gas, so it can be measured and used as work function sensors [12-14].

Rakib Hossain *et al.* investigated the behavior of (chlor-methine anticancer drug) on the surface of three different nanoparticles to understand the adsorption properties of CM

drug over these nanoparticles and find a suitable drug delivery system. They have investigated the adsorption behavior of CM drug with the surface of C_{24} , $B_{12}C_6N_6$, and $B_{12}N_{12}$ nanocages by using DFT calculation. It has been observed that the CM molecule was adsorbed on the C_{24} and $B_{12}C_6N_6$ nanostructures with unfavorable adsorption energy [15].

Also, in 2020, Rakib Hossain *et al.* made a DFT and QAIM investigations of the adsorption of chlormethine anticancer drug on the exterior surface of pristine and transition metal functionalized boron nitride fullerene. They proved that the f-BN nanostructures show a better reactivity than the pristine BN nanocage with enhanced the dipole moment value enables them to perform more intensive interaction with the CM drug [16].

On the other hand, Rakib Hossain *et al.* introduced a comparative DFT and QAIM insight study on the adsorption behavior of metronidazole (ML) drug molecules on the surface of hydrogenated graphene (h-GN), boron nitride (BN), and boron carbide (BC) nanosheets in a gaseous and aqueous medium, and they observed that ML drug molecule shows different interactions phenomena with h-GN, BN and BC nanosheets because these adsorbent sheets possess diverse structural, thermo-dynamical, electronic and optical properties, and realized the electron sharing between the molecules at BCPs. In that work, QAIM analysis indicates the weak electrostatic interactions between ML and nanosheets which are in excellent agreement with weak physisorption adsorption [17].

In 2001, Qiao and coworkers reported UV/Vis absorption, fluorescence spectra, and dynamic study on interactions of C_{60} with eight kinds of aliphatic amines, such as di-ethylamine and triethylamine tri-*n*-amyl amine, propyl ethylamine, *n*-butylamine, *n*-heptylamine, dodecyl amine, and ethylenediamine [18]. They showed that charge-transfer interactions of C_{60} with aliphatic amines are much stronger than that of C_{60} with aromatic amines, and the products can all emit a strong fluorescence at the relatively shorter wavelength around 519 nm.

Kushwaha *et al.* introduced a review study on carbon nanotubes as a novel drug delivery system for anticancer therapy. They proved that the issues surrounding CNT toxicity remain inconclusive, as numerous conflicting studies demonstrate both toxic and nontoxic behavior despite several drugs delivered using carbon nanotubes. Still, also it is an extremely promising application of nano-technology. It is definitely worth further research, as the current methods for cancer treatment are indiscriminately harmful and only partially effective [19].

Saleh and coworkers studied on the adsorption of metformin (MF) drug on the Si and Al doped (5,5) single wall carbon nanotube (SWCNT). They noticed that the nature of MF adsorption was high chemisorption. MF drug provided stronger adsorption on Al-doped SWCNT than that of the Si-doped one. They have proposed that Si-doped (5,5) SWCNT can be extended as a drug delivery system instead of Al-doped (5,5) SWCNT [20].

Bagheri Novir *et al.* made quantum mechanical studies of the adsorption of Remdesivir®, as an effective drug for the treatment of COVID-19 on the surface of pristine, COOH-functionalized, and S-, Si- and Al-doped (5,5) SWCNT. Also, they concluded that the Si-doped CNT is the best nano vehicle for Remdesivir® drug delivery compared to the pristine CNT and the other functionalized and doped CNTs investigated in this study because of its better reactivity, better energetic, electronic, adsorption, and thermodynamic properties [21].

Recently, interactions between nanotubes and ligands have become an important subject, and they can be used together as drug delivery agents and sensors [22-26]. The binding energy values of the Al-CNT suggest that doping of nanotube enhances the interaction mechanism and alters the structural, chemical,

and electronic properties of the complexes. When the Al-doped atom interacts with the active atoms of the BMSF-BENZ, the complexes become more stable, leading the binding energies to lie in the range of chemisorption [27]. To the best of the author's acquaintance, there is no previously done comparative investigation about the adsorption of the BMSF-BENZ on Al-CNT (4,0) SWCNT or Al-CNT (6,0). Our main objective is to explore the adsorption behavior of BMSF-BENZ on the surface of zigzag Al-CNT (n,0) SWCNT. For this purpose, we have a comparative investigation of various structural and electronic properties before and after the adsorption of BMSF-BENZ on the nanotube.

2. Computational methods

All calculations were carried out by using Density Functional Theory (DFT) with B3LYP and 6-31G(d,p) basis set as employed in Gaussian 09 package [28]. In this work, the vibrational frequencies for all new complexes with the original compounds were analyzed to check the true global minima of our predicted Al-CNT Nanotubes. Then, the BMSF-BENZ was adsorbed. Adsorption energy, charge transfer analysis, change in energy gap, dipole moment, and recovery time were also examined to predict the interaction between the drug molecule with nanoparticles.

Electronegativity can be calculated from E_{HOMO} and E_{LUMO} using the Equation (1) [29].

$$\chi = -\frac{1}{2} (E_{HOMO} + E_{LUMO}) \quad (1)$$

To investigate the effect of BMSF-BENZ on the Fermi level energies and work function of the nanotube, Fermi level energy was calculated by using the Equation (2) for electronegativity, Fermi energy can be estimated such that $E_f = -\chi$ [30].

$$E_f = E_{HOMO} + \left(\frac{E_{LUMO} - E_{HOMO}}{2} \right) \quad (2)$$

Several calculations were executed to calculate the total energies of the molecules depending on the position of the nanotube attached to the drug molecule. The adsorption energies of drug on the surfaces of the nanotubes were obtained by Equation (3) [31,32].

$$E_{ads} = E_{complex} - (E_{nanotube} + E_{drug}) \quad (3)$$

where $E_{complex}$, $E_{nanotube}$ and E_{drug} donate the energy of the complex composed with nanotubes drug and isolated energies of nanotube and drug, respectively. The E_{ads} energy was determined from the summation of the interaction energy (E_{int}) and deformation energies (E_{def}) of the drug ($E_{def-drug}$) and nanotubes ($E_{def-nanotube}$) during the adsorption process [33].

$$E_{int} = E_{complex} - (E_{nanotube\ in\ complex} + E_{drug\ in\ complex}) \quad (4)$$

$$E_{def} = (E_{drug\ in\ complex} - E_{drug}) + (E_{nanotube\ in\ complex} - E_{nanotube}) \quad (5)$$

where $E_{nanotube\ in\ complex}$, $E_{drug\ in\ complex}$ are the energies of nanotube and drug with their geometries in the complex, respectively.

The thermodynamical parameters were also investigated such as changes of Gibbs free energy (ΔG), entropy (ΔS), and enthalpy (ΔH), to check the structural stability [30] by using the Equations (6-8) [34].

$$\Delta G = G_{complex} - G_{nanotube} - G_{drug} \quad (6)$$

$$\Delta H = H_{complex} - H_{nanotube} - H_{drug} \quad (7)$$

$$\Delta S = \frac{\Delta H - \Delta G}{T} \quad (8)$$

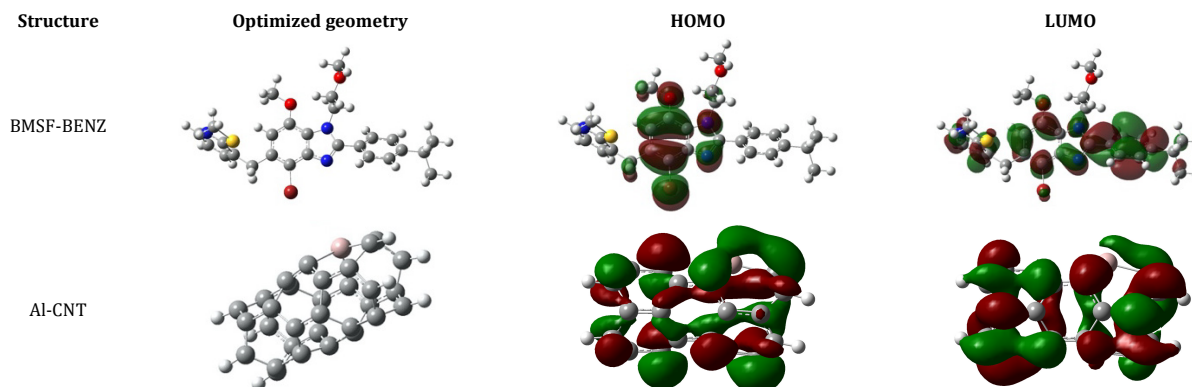


Figure 1. Optimized geometries, HOMO, LUMO of the BMSF-BENZ drug, Al-CNT.

where G_{complex} and H_{complex} are the Gibbs free energy and the enthalpy of drug adsorbed upon nanotubes, G_{nano} and H_{nano} are the Gibbs free energy and enthalpy of the nanotubes and G_{drug} and H_{drug} are the Gibbs free energy and enthalpy of the drug respectively. T is the room temperature equal to 298.15 K.

Quantum Theory of Atoms in Molecules (QTAIM) analysis based on Bader's [35] has evaluated by MULTIWFN program [36] in order to understand the nature of interactions between drug molecule and Al-CNT material. Density of States (DOS) analysis has also been obtained by MULTIWFN 3.7 program [37]. Recovery time has studied to predict the desorption process of the drug molecule from Al-CNT surfaces when the adsorbents in the gas phase.

3. Results and discussions

3.1. Optimized geometry of the adsorbents

An adsorbent nanotube of zigzag Al-doped SWCNT (n,0) was considered for the BMSF-BENZ drug as an osteoporosis disease drug delivery vehicle. Initially, the nanotube and BMSF-BENZ molecule were optimized using DFT calculation in a gas media. The optimized geometries of adsorbent Al-CNT and drug molecules with their corresponding HOMO, LUMO are shown in Figure 1.

The vibrational modes for the new complexes and the original compounds were investigated to verify the structural stability in the presence of IR. All compounds give vibrational modes in a positive frequency range of 9.49, 9.58, 9.53, 4.65, 5.03, 2.87, 7.97 cm^{-1} as a minimum value, and 3248.12, 3248.10, 3244.93, 3243.82, 3245.85, 3222.02, 3224.24 cm^{-1} as a maximum value for the active atom binding Br, N₈, N₉, N₅₈, O₃₅, O₄₁, and S with Al-CNT nanotube. Furthermore, the HOMO and LUMO energies were also calculated to find the energy gap of nanotubes. HOMO levels are located on C-C bonds throughout one side of the nanotube, whereas LUMO levels were located on the C-C bonds opposite side of the nanotube. The predicted energy gap of Al-CNT 1.76, 1.73, 1.75, 1.52, 1.76, 1.75 and 1.74 eV for all locations, respectively.

3.2. BMSF-BENZ adsorption on Al-CNT nanotube

To find suitable adsorbents for BMSF-BENZ, we have tried to investigate different properties such as geometric, electronic, and adsorption properties, etc., of BMSF-BENZ/Al-CNT complexes. Initially, the BMSF-BENZ was adsorbed on different adsorption sites of the Al-CNT nanotube and found the preferable adsorption site at the Al atom where the Br, N₈, N₉, N₅₈, O₃₅, O₄₁, and S atoms of the BMSF-BENZ get close to the surface of the Al-CNT nanotube. In the case of the BMSF-BENZ adsorbed complex, the geometry of the Al-CNT remains

unchanged, and bond lengths of C-C varied about ~ 0.03 Å at the nearby adsorption site. It claims that there is an interaction between BMSF-BENZ and Al-CNT nanotubes, and it was confirmed by adsorption energy and changes in electronic properties analysis. BMSF-BENZ drug molecule was adsorbed on the Al-CNT nanotube with adsorption energy about -22.09, -38.68, -12.89, -31.01, -27.31, -21.90 and -21.42 kcal/mol at a minimum distance of about 2.54, 2.01, 2.17, 2.03, 1.95, 1.96 and 2.48 Å at the B3LYP method as shown in Table 1. In order to analyze the adsorption and desorption process together, the charging Q (e) values of Al-CNT by adsorption process and the recovery time were obtained in vacuum UV light conditions with frequency $3 \times 10^{16} \text{ s}^{-1}$ at room temperature for the different complexes in the gas phase have given in Table 1.

In order to understand the nature of the interactions of BMSF-BENZ drug on Al-CNTs, Topology Analysis based on Bader's quantum theory of atoms in molecules method has been employed with the MULTIWFN program [36]. It has applied the N₅₈/Al-CNT complexes with the negative adsorption energy and extended recovery time values given in Table 1. The nature of intermolecular interactions between the drug and Al-CNT is determined by topology parameters which are calculated in terms of electron density at critical bond points (BCPs) using QTAIM analysis and given in Table 2. The N₅₈/Al-CNT complex was selected as a good sample to demonstrate that it has reasonably strong interactions causing the highest percentage variation of band gap given in Table 3.

In QTAIM analysis, mostly, the electron density of $\rho(r)$ and Laplacian $\nabla^2\rho(r)$ characteristics are widely used to understand the bonding interactions nature. However, the total energy density of H(r) and the ratio of $|V(r)|/(G(r))$ are more remarkable parameters on bonding characteristics. It has been noted that for weak and medium-strength hydrogen bonding and Van der Waals interactions due to $\nabla^2\rho(r) > 0$, $H(r) > 0$, $|V(r)|/(G(r)) < 1$. The strong hydrogen bonds as the intermediate type of interaction related to $\nabla^2\rho(r) > 0$, $H(r) < 0$, $(1 < |V(r)|)/(G(r)) < 2$. The covalent bonding characteristics correspond to $\nabla^2\rho(r) < 0$, $H(r) < 0$, $|V(r)|/(G(r)) > 2$.

The calculated QTAIM parameters for the complex structure of N₅₈/Al-CNT are illustrated in Table 2, and the interaction between the drug and Al-CNT is also shown in Figure 2. The computed molecular topographical map of the BMSF-N₅₈/Al-CNT complex with critical points and atom labels is also illustrated in Figure 2. From the computation results given in Table 2, there are four typical interactions between the drug and Al-CNT. The interaction of N41 and Al26 atoms can be classified as intermediate interaction as the semi-covalent character due to $\nabla^2\rho(r) > 0$, $H(r) < 0$, $(1 < |V(r)|)/(G(r)) < 2$ rule. The other three QTAIM parameters correspond to weak hydrogen bonding interactions because the topology parameters reveal only the electrostatic nature of those bonds.

Table 1. The adsorption energy (E_{ads}) for B3LYP functional in kcal/mol, the minimum distance between BMSF-BENZ molecule, and adsorbents (d) in Å, Bond length between active atoms of the nanotubes after adsorption of BMSF-BENZ drug for the different complex in gas phase, the Q_{Al-CNT} denotes the charge values of Al-CNT in e and recovery time (τ) in sec.

Structure	d	E_{ads}	Bond location	Bond length after adsorption	Q_{Al-CNT} (e)	τ (sec)
BMSF-BENZ	-	-	-	-	-	-
Al-CNT	-	-	-	-	-	-
Br/Al-CNT	2.54	-22.09	Al-C1	1.92	-0.2804	0.537
			Al-C2	1.94		
			Al-C3	1.94		
N_8 /Al-CNT	2.01	-38.68	Al-C1	1.94	-0.3382	1.77×10^{12}
			Al-C2	1.97		
			Al-C3	1.98		
N_9 /Al-CNT	2.17	-12.89	Al-C1	1.92	-0.1734	9.92×10^{-8}
			Al-C2	1.95		
			Al-C3	1.96		
N_{58} /Al-CNT	2.03	-31.01	Al-C1	1.93	-0.2566	6.71×10^6
			Al-C2	1.97		
			Al-C3	1.96		
O_{35} /Al-CNT	1.95	-27.31	Al-C1	1.93	-0.2113	1.75×10^4
			Al-C2	1.95		
			Al-C3	1.95		
O_{41} /Al-CNT	1.96	-21.90	Al-C1	1.92	-0.1999	6.94×10^1
			Al-C2	1.95		
			Al-C3	1.95		
S/Al-CNT	2.48	-21.42	Al-C1	1.93	-0.2971	3.05×10^{-1}
			Al-C2	1.96		
			Al-C3	1.95		

Table 2. The QTAIM parameters of the selected N_{58} /Al-CNT complex at the BCPs. Electron density ($\rho(r)$), Laplacian of electron density ($\nabla^2\rho(r)$), the kinetic electron density ($G(r)$), potential electron density ($V(r)$), total electron energy density ($H(r)$), the ratio $|V_{BCP}|/G_{BCP}$.

Structure	BCP Drug/Al-CNT	ρ_{BCP}	$\nabla^2\rho_{BCP}$	G_{BCP}	V_{BCP}	H_{BCP}	$ V_{BCP} /G_{BCP}$
N_{58} /Al-CNT	N_{41} - Al_{26}	0.0527998	0.2739379	0.0688833	-0.0692820	-0.398775×10^{-3}	1.0057880
	H_{57} - C_{17}	0.0081556	0.0245705	0.0049469	-0.0037512	0.0011957	0.7582931
	H_{74} - C_{25}	0.0019901	0.0049537	0.9144×10^{-3}	-0.5904×10^{-3}	0.324009×10^{-3}	0.6456693
	H_{93} - H_{39}	0.8760×10^{-6}	0.950×10^{-5}	0.1389×10^{-5}	-0.4039×10^{-6}	0.985723×10^{-6}	0.2907847

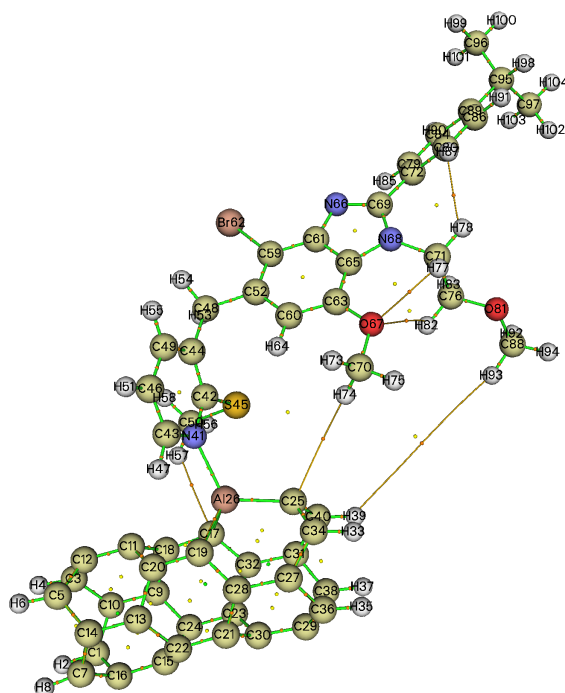


Figure 2. The computed molecular topographical map of BMSF- N_{58} /Al-CNT complex with all critical points. Atomic and bond critical points are presented by atom labels and orange spheres, respectively. The cage and ring critical points due to green and yellow circles. The lines are bond paths.

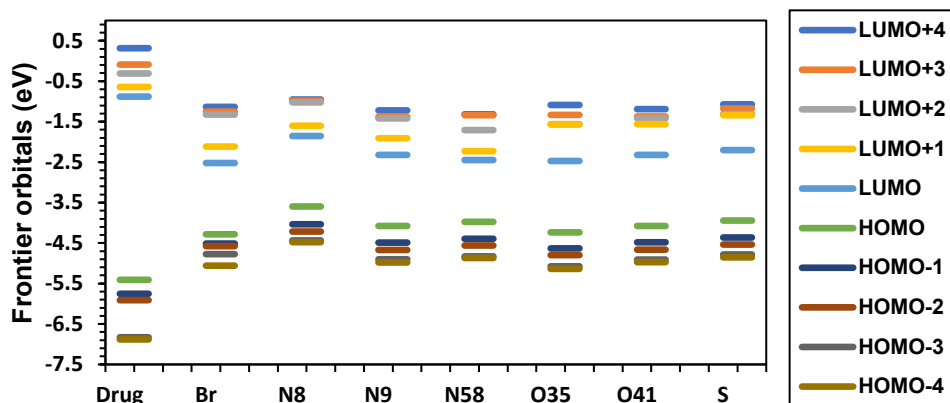
The quantum descriptors of BMSF-BENZ /Al-CNT complex structures denoted by Equations (1-4) are calculated and given in Table 3. In the BMSF-BENZ/Al-CNT structure, the electronic parameters such as E_{HOMO} , E_{LUMO} , E_g , and Fermi level energies have a noticeable change. The values of E_{HOMO} and E_{LUMO} of Al-CNT nanotubes before the adsorption of molecules are -4.63 and -2.88 eV, and after adsorption of BMSF-BENZ drug are mentioned in Table 3. The sensors are related to the variation

of their electrical conductance after drug adsorption due to the electron exchange between the drug and sensor. On this line, the CNT sensitivity to the drug is based on the changing of HOMO and LUMO energies with ΔE_g .

In order to understand the sensing mechanism of the Al-CNT to drug, the percentage variation of % ΔE_g gap during the adsorption process is taken into account by the following equation:

Table 3. Calculated HOMO energy (E_{HOMO}), LUMO energy (E_{LUMO}), HOMO-LUMO energy gap (E_g), Fermi level energy (E_f), and Φ of the studied complexes. All data are in the unit of eV.

Structure	E_{HOMO}	E_{LUMO}	E_g	$\% \Delta E_g$	E_f	Φ	$\% \Delta \Phi$
Benzimidazole	-5.40	-0.88	4.52	-	-3.14	3.14	-
Al-CNT	-4.63	-2.88	1.74	-	-3.76	3.76	-
Br/Al-CNT	-4.28	-2.52	1.76	1.29	-3.40	3.40	-9.47
N ₈ /Al-CNT	-3.59	-1.85	1.73	-0.14	-2.72	2.72	-13.29
N ₉ /Al-CNT	-4.08	-2.32	1.75	0.96	-3.20	3.20	17.38
N ₅₈ /Al-CNT	-3.97	-2.45	1.52	-12.31	-3.21	3.21	0.41
O ₃₅ /Al-CNT	-4.23	-2.47	1.76	1.29	-3.35	3.35	4.31
O ₄₁ /Al-CNT	-4.07	-2.32	1.75	0.95	-3.19	3.19	-4.59
S/Al-CNT	-3.94	-2.20	1.74	0.17	-3.07	3.07	-3.87

**Figure 3.** Energy gap between HOMO and LUMO for BMSF-BENZ drug, Al-CNT nanotube, with all investigated locations regarding to the position of the nanotube on the drug.

$$\% \Delta E_g = 100x(\Delta E_{g2} - \Delta E_{g1})/\Delta E_{g1} \quad (9)$$

where ΔE_{g1} and ΔE_{g2} are the ΔE_g values of CNT and complex structure, respectively. The percentage change values, of $\% \Delta E_g$ for each structure are given in Table 3.

The corresponding frontier molecular orbital map is shown in Figure 3, and the Frontier molecular orbital (HOMO and LUMO) of all investigated complexes is shown in Figures 4 and 5. Thus, the BMSF-BENZ drug molecule was significantly affecting the HOMO energy level and LUMO energy level as shown in Table 3.

As reported energies of E_{HOMO} and E_{LUMO} and energy gap (E_g) in Table 3, some electronic properties of Al-CNT are affected weakly by the adsorption of the BMSF-BENZ drug. The decreasing order of percentage change values are obtained for the interactions of N₈ and N₅₈ atoms of the BMSF-BENZ drug with Al-CNT as -0.14%, -12.31%, but for other atoms of Br, N₉, O₃₅, O₄₁, and S are about 1.29, 0.96, 1.29, 0.95, and 0.17% by increasing, respectively.

It is known that the lower E_g values indicate higher electrical conductivity, reactivity, and sensitivity. Therefore, decreasing the E_g through adsorption of the BMSF-BENZ drug molecule indicates that the Al-CNT can detect the drug. Thus, among all studied geometries of complex structures, the highest variation value of $\% \Delta E_g$ has been obtained by the N₅₈ atom of the BMSF-BENZ interacts with Al-CNT nanotube.

According to the values of percentage variation of the work function of $\% \Phi$, the structure corresponding to N₉/Al-CNT has the highest value of 17.38% by increasing the conduction electrons. That complex structure can be used as a work function type sensor because of the short recovery time of 9.92×10^{-8} sec given in Table 1. The Br/Al-CNT complex structure has the decreasing percentage variation value of 9.47% in the work function. The Br/Al-CNT complex structure may candidate as a work function sensor too with the reasonable recovery time of 0.537 sec. The increasing variation of the work function for O₃₅/Al-CNT complex structure is about

4.31%. However, it has long recovery time of 17500sec. The O₄₁/Al-CNT and S/Al-CNT complex structures have the percentage variation values of 4.59 and 3.87% by decreasing the work function, respectively. Those complex structures are considered as work function type sensors with short recovery time values of 0.694 sec and 0.305 sec for O₄₁/Al-CNT and S/Al-CNT, respectively.

The density of states (DOS) diagram of the complex structure of N₅₈ atom of the BMSF-BENZ interacting with Al-CNT was selected to plot in Figure 6 because of the significant $\% \Delta E_g$ values given in Table 3, each was also calculated in order to better understand the stability of the system. The change in E_g by DOS analysis can be confirmed as shown in Figure 6 by MULTIWFN program [37].

It is clear in Figure 6 that the bandgap of the complex is getting narrow concerning the E_g of Al-CNT. An important parameter used for gas sensors and drug delivery systems is the recovery time or the desorption time, which predicts the amount of time required to desorb the drug from the adsorbents. This parameter is exponentially related to the adsorption energy, and high adsorption interaction needs a high desorption time, and low interaction requires a low desorption time. The recovery time is calculated by the Equation (10) [38].

$$\tau = \frac{1}{\vartheta} \exp\left(\frac{-E_{\text{Ads}}}{KT}\right) \quad (10)$$

where temperature and the attempt frequency are defined by T in K and ϑ , respectively. K is Boltzmann's constant ($\sim 2 \times 10^{-3}$ Kcal/mol.K).

As the BMSF-BENZ molecule seems to be adsorbed on the Al-CNT nanotube with maximum adsorption energy, a different recovery time (Table 1) was obtained in vacuum UV- light conditions with frequencies of 3×10^{16} sec⁻¹ at room temperature. When the adsorption energy is more than 1 eV (23.061 kcal/mol) (in magnitude), a strong chemical interac-

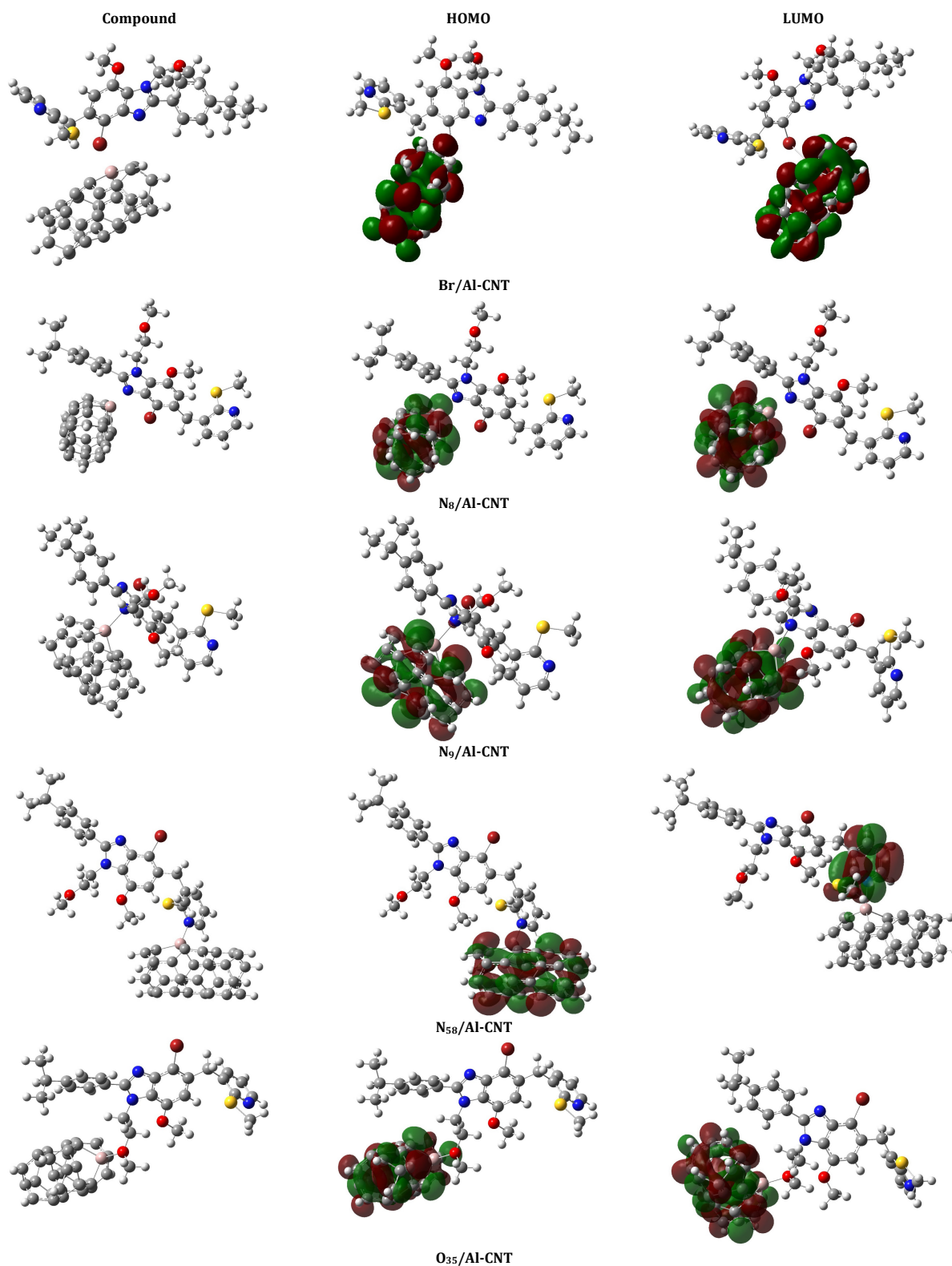


Figure 4. The Frontier molecular orbital (HOMO and LUMO) of Br/Al-CNT, N₈/Al-CNT, N₉/Al-CNT, N₅₈/Al-CNT and O₃₅/Al-CNT. The considered iso value is 0.02 electron/bohr³.

tion between adsorbate and adsorbent is considered to occur, and the adsorption process is then levelled as chemisorption. Therefore, the more negative the adsorption energy, the more strongly the system is connected, representing a higher stable system. Therefore, for drug delivery and drug sensor devices,

the adsorption process between drug molecules and adsorbents is expected to negatively value adsorption energy. In drug delivery systems, the adsorbent must have a strong interaction with the drug. However, for drug sensor devices, there should be a lower energy interaction [39].

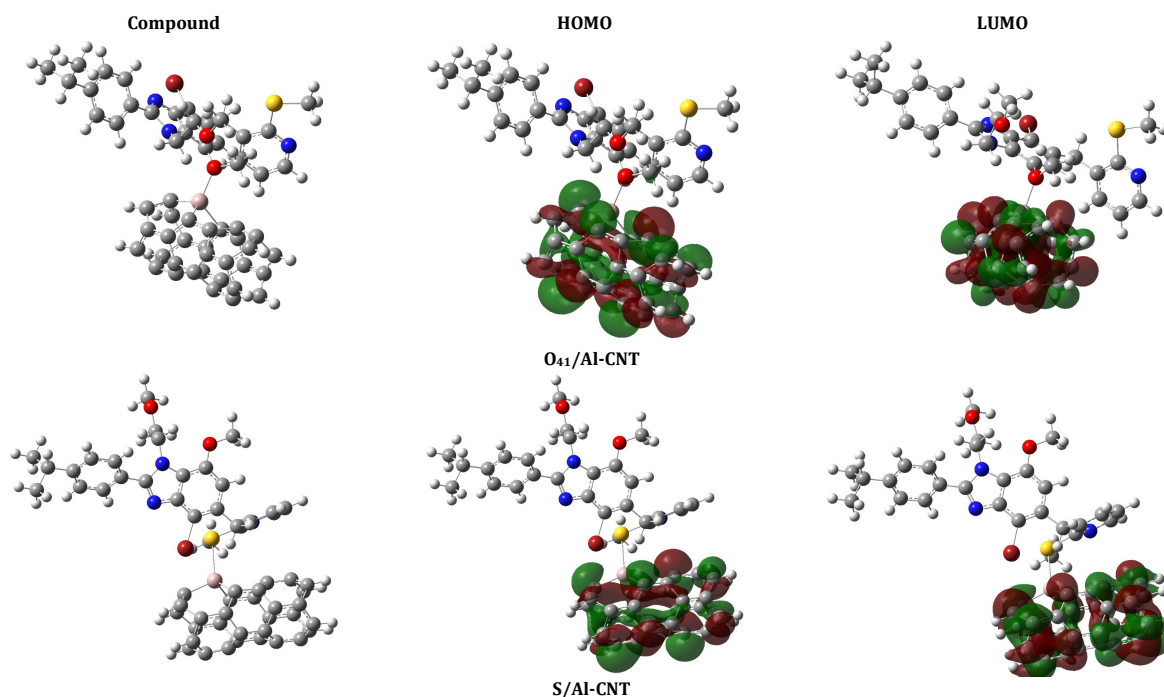


Figure 5. The Frontier molecular orbital (HOMO and LUMO) of $O_{41}/Al-CNT$ and $S/Al-CNT$. The considered iso value is 0.02 electron/bohr³.

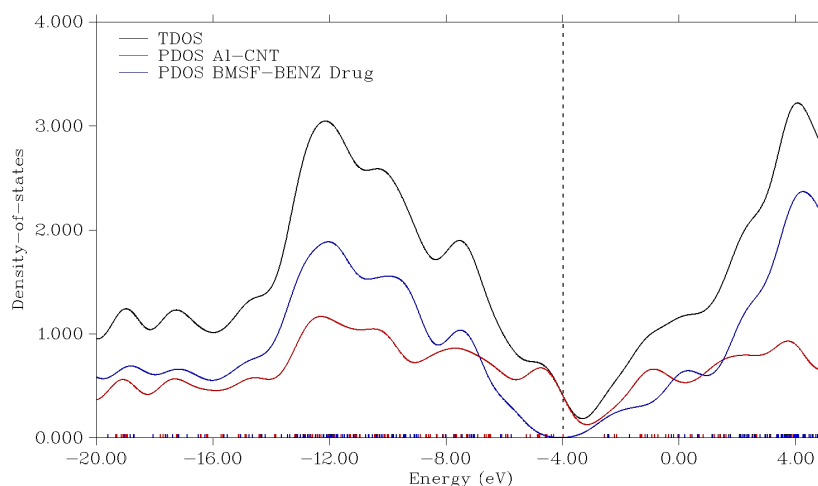


Figure 6. TDOS and PDOS plots for complex structure of $N_{58}-BMSF-BENZ /Al-CNT$. The dashed line shows the HOMO energy level.

On this line, the adsorption process for $Br/Al-CNT$, $O_{41}/Al-CNT$ and $S/Al-CNT$ complexes are physisorption with the lower E_{ads} energy values of -0.958, -0.949, -0.929 eV than 1 eV, respectively. By combining the corresponding recovery time values of those complexes in Table 1 with the percentage variation of work function given in Table 3, it has been evaluated that those complexes can be used as an amperometric drug sensor applications of BMSF-BENZ drug molecule on Al-CNT nanotube.

Despite this most stable and sensible interaction, the N_9 atom of the BMSF-BENZ molecule and Al-CNT nanotube suffer from a considerable short recovery time. However, the strong interactions with considerable negative adsorption energies for the complex structures of $N_8/Al-CNT$, $N_{58}/Al-CNT$ and $O_{35}/Al-CNT$ have obtained as -1.677, -1.345 and -1.184 eV. Those values indicate that the adsorption process of $N_8/Al-CNT$, $N_{58}/Al-CNT$ and $O_{35}/Al-CNT$ complexes are in chemisorption nature with the desorption time values of 1.77×10^{12} , 6.71×10^6 and 1.75×10^4 sec, respectively. Among them, the complex of

$O_{35}/Al-CNT$ can be extended as drug delivery system with reasonable recovery time of 12 days.

The adsorbate-adsorbent distance with the adsorption energy and a reasonable amount of charge transfer from the BMSF-BENZ molecule to the nanotube demonstrates that combining the drug with the complex is possible in all locations of the active atoms of the BMSF-BENZ molecule. The charge transfer from BMSF-BENZ molecule to the Al-CNT nanotube for Br, N_8 , N_9 , N_{58} , O_{35} , O_{41} , S atoms of BMSF-BENZ molecule are 0.2804, 0.3382, 0.1734, 0.2537, 0.2113, 0.1999, 0.2971 e⁻, respectively, indicates the most significant charge transfer occurs from N_8 atom belonging to BMSF-BENZ molecule to the Al-CNT nanotube.

To understand the thermodynamic stability of the complexes, we also investigated the thermodynamic parameters such as the change in enthalpy (ΔH), Gibbs free energy (ΔG), and entropy (ΔS) by using Equations (6-8), and the values are mentioned in Table 4.

Table 4. The change of Gibbs free energy (ΔG) in kcal/mol, change of enthalpy (ΔH) in kcal/mol, and change of entropy (ΔS) in kcal/mol.K, minimum and maximum frequency in cm^{-1} for the different complexes in gas phase.

No	Structure	ΔG	ΔH	ΔS	V_{min}	V_{max}
1	Br/Al-CNT	-11.00	-22.71	-0.03	9.49	3248.12
2	N_8 /Al-CNT	-34.06	-48.30	-0.04	9.58	3248.10
3	N_9 /Al-CNT	-9.44	-23.28	-0.04	9.53	3244.93
4	N_{58} /Al-CNT	-29.65	-41.78	-0.04	4.65	3243.82
5	O_{35} /Al-CNT	-21.20	-32.61	-0.03	5.03	3245.85
6	O_{41} /Al-CNT	-17.66	-30.02	-0.04	2.87	3222.02
7	S/Al-CNT	-12.32	-25.93	-0.04	7.97	3224.24

The positive values of ΔH and ΔG represent that the reaction process is endothermic and non-spontaneous. In contrast, the negative values of ΔH and ΔG indicate the reaction is an exothermic and spontaneous process [40].

The obtained data of ΔH and ΔG were negative values in all investigated complexes, i.e., these complexes are thermodynamically stable, and the more negative value of ΔS means the more ordered complex. Therefore, the thermodynamic parameters predict that the investigated complexes are more favorable and thermodynamic stable for BMSF-BENZ drug delivery.

4. Conclusions

To find a suitable delivery method for the BMSF-BENZ drug, we have investigated the adsorption behavior of the BMSF BENZ drug on the surface of Al-CNT by using DFT calculation. It has been observed that the BMSF-BENZ molecule was adsorbed on the nanostructures with different adsorption energy depending on the location of the nanotube to the active atoms of the drug. The HOMO energy, LUMO energy, HOMO-LUMO energy gap, and Fermi level energies were after adsorption of the BMSF-BENZ drug on the nanoparticles' nanoparticles adsorbing BMSF-BENZ on the Al-CNT nanotube. The BMSF-BENZ drug was adsorbed on the Al-CNT nanotube with an adsorption energy of -22.09, -38.68, -12.89, -31.01, -27.31, -21.90, and -21.42 kcal/mol in the gas phase at the B3LYP method, which is more favorable for the drug delivery system and work function type sensor applications. Br/Al-CNT, O_{41} /Al-CNT and S/Al-CNT complexes are physisorption nature to be used work function type drug sensor, while O_{35} /Al-CNT can be extended as drug delivery system. Furthermore, the Gibbs free energy demonstrates that BMSF-BENZ /Al-CNT configuration shows spontaneous and favorable adsorption energy. Therefore, we could suggest that the Al-CNT nanotube would be a promising drug delivery vehicle for BMSF-BENZ drug molecules. QTAM analysis was carried out for N_{58} /Al-CNT complex and found that The interaction of N_{41} and Al_{26} atoms can be classified as intermediate interaction as the semi-covalent character due to $V^2\rho(r) > 0$, $H(r) < 0$, ($1 < |V(r)|/G(r) < 2$) the rule and this is most stable and sensible for the interaction N_8 atom of BMSF-BENZ molecule, but Al-CNT nanotube suffers from a considerable recovery time.

Disclosure statement

Conflict of interests: The authors declare that they have no conflict of interest.

Author contributions: All authors contributed equally to this work.

Ethical approval: All ethical guidelines have been adhered.

Sample availability: Samples of the compounds are available from the author.

ORCID

Zaid Husham Al-Sawaff

 <https://orcid.org/0000-0001-8789-4905>

Serap Senturk Dalgic

 <https://orcid.org/0000-0003-2541-9214>

Fatma Kandemirli

 <https://orcid.org/0000-0001-6097-2184>

References

- [1]. Kanis, J. A.; Cooper, C.; Rizzoli, R.; Reginster, J.-Y. *Osteoporos. Int.* **2020**, *31* (1), 209.
- [2]. Deal, C. *Nat. Clin. Pract. Rheumatol.* **2009**, *5* (1), 20–27.
- [3]. Shimizu, M.; Noda, H.; Joyashiki, E.; Nakagawa, C.; Asanuma, K.; Hayasaka, A.; Kato, M.; Nanami, M.; Inada, M.; Miyaura, C.; Tamura, T. *Biol. Pharm. Bull.* **2016**, *39* (4), 625–630.
- [4]. Mias, S.; Sudor, J.; Camon, H. *Microsyst. Technol.* **2008**, *14*, 747–751.
- [5]. Gu, M.; Zhang, Q.; Lamon, S. *Nat. Rev. Mater.* **2016**, *1* (12) 1–14. <https://doi.org/10.1038/natrevmats.2016.70>.
- [6]. Varghese, S. S.; Lonkar, S.; Singh, K. K.; Swaminathan, S.; Abdala, A. *Sens. Actuators B Chem.* **2015**, *218*, 160–183.
- [7]. Rad, A. S.; Ayub, K. *J. Alloys Compd.* **2016**, *678*, 317–324.
- [8]. Pannopar, P.; Khongpracha, P.; Probst, M.; Limtrakul, J. *J. Mol. Graph. Model.* **2009**, *28* (1), 62–69.
- [9]. Conti, M.; Tazzari, V.; Baccini, C.; Pertici, G.; Serino, L. P.; De Giorgi, U. *In Vivo* **2006**, *20* (6A), 697–701.
- [10]. Singh, R.; Lillard, J. W., Jr. *Exp. Mol. Pathol.* **2009**, *86* (3), 215–223.
- [11]. Bakry, R.; Vallant, R. M.; Najam-ul-Haq, M.; Rainer, M.; Szabo, Z.; Huck, C. W.; Bonn, G. K. *Int. J. Nanomedicine* **2007**, *2* (4), 639–649.
- [12]. Zhang, T.; Mubeen, S.; Myung, N. V.; Deshusses, M. A. *Nanotechnology* **2008**, *19* (33), 332001.
- [13]. Snow, E. S.; Perkins, F. K.; Robinson, J. A. *Chem. Soc. Rev.* **2006**, *35* (9), 790–798.
- [14]. Giannozzi, P. *Appl. Phys. Lett.* **2004**, *84* (19), 3936–3937.
- [15]. Rakib Hossain, M.; Mehade Hasan, M.; Ud Daula Shamim, S.; Ferdous, T.; Abul Hossain, M.; Ahmed, F. *Comput. Theor. Chem.* **2021**, *1197* (113156), 113156.
- [16]. Hossain, M. R.; Hasan, M. M.; Nishat, M.; Noor-E-Ashrafi; Ahmed, F.; Ferdous, T.; Hossain, M. A. *J. Mol. Liq.* **2021**, *323* (114627), 114627.
- [17]. Hossain, M. R.; Hasan, M. M.; Ashrafi, N. E.-.; Rahman, H.; Rahman, M. S.; Ahmed, F.; Ferdous, T.; Hossain, M. A. *Physica E Low Dimens. Syst. Nanostruct.* **2021**, *126* (114483), 114483.
- [18]. Qiao, J. L.; Gong, Q. J.; Du, L. M.; Jin, W. J. *Spectrochim. Acta A Mol. Biomol. Spectrosc.* **2001**, *57* (1), 17–25.
- [19]. Kushwaha, S. K. S.; Ghoshal, S.; Rai, A. K.; Singh, S. *Braz. J. Pharm. Sci.* **2013**, *49* (4), 629–643.
- [20]. Hoseiniezahad-Namin, M. S.; Pargolghasemi, P.; Alimohammadi, S.; Rad, A. S.; Taqavi, L. *Physica E Low Dimens. Syst. Nanostruct.* **2017**, *90*, 204–213.
- [21]. Bagheri Novir, S.; Aram, M. R. *Physica E Low Dimens. Syst. Nanostruct.* **2021**, *129* (114668), 114668.
- [22]. Shi, J.; Wang, B.; Wang, L.; Lu, T.; Fu, Y.; Zhang, H.; Zhang, Z. *J. Control. Release* **2016**, *235*, 245–258.
- [23]. Afshari, T.; Mohsennia, M. *Mol. Simul.* **2019**, *45* (16), 1384–1394.
- [24]. Parlak, C.; Alver, Ö.; Ramasami, P. *Main Group Met. Chem.* **2016**, *39* (5–6) 145–150. <https://doi.org/10.1515/mgmc-2016-0031>
- [25]. Bashiri, S.; Vessally, E.; Bekhradnia, A.; Hosseini, A.; Edjlali, L. *Vacuum* **2017**, *136*, 156–162.
- [26]. Parlak, C.; Alver, Ö.; Şenyel, M. *J. Theor. Comput. Chem.* **2017**, *16* (02), 1750011.
- [27]. Bilge, M. *Anadolu Univ. J. Sci. Technol.-Appl. Sci. Eng.* **2017**, 1–1.
- [28]. Frisch, M. J.; Trucks, G. W.; Schlegel, H. B.; Scuseria, G. E.; Robb, M. A.; Cheeseman, J. R.; Scalmani, G.; Barone, V.; Mennucci, B.; Petersson, G. A.; Nakatsuji, H.; Caricato, M.; Li, X.; Hratchian, H. P.; Izmaylov, A. F.; Bloino, J.; Zheng, G.; Sonnenberg, J. L.; Hada, M.; Ehara, M.; Toyota, K.; Fukuda, R.; Hasegawa, J.; Ishida, M.; Nakajima, T.; Honda, Y.; Kitao, O.; Nakai, H.; Vreven, T.; Montgomery, J. A.; Peralta, J. E.; Ogliaro, F.; Bearpark, M.; Heyd, J. J.; Brothers, E.; Kudin, K. N.; Staroverov, V. N.; Kobayashi, R.; Normand, J.; Raghavachari, K.; Rendell, A.; Burant, J. C.; Iyengar, S. S.; Tomasi, J.; Cossi, M.; Rega, N.; Millam, J. M.; Klene, M.; Knox, J. E.; Cross, J. B.; Bakken, V.; Adamo, C.; Jaramillo, J.; Gomperts, R.; Stratmann, R. E.; Yazyev, O.; A. J. Austin, A. J.; Cammi, R.; Pomelli, C.; Ochterski, J. W.; Martin, R. L.; Morokuma, K.; Zakrzewski, V. G.; Voth, G.

- A.; Salvador, P.; Dannenberg, J. J.; Dapprich, S.; Daniels, A. D.; Farkas, O.; Foresman, J. B.; Ortiz, J. V.; Cioslowski, J.; Fox, D. J. Gaussian, Inc., Gaussian 09, Revision D.01, Wallingford CT, 2013.
- [29]. Kim, T.; Ri, C.; Yun, H.; An, R.; Han, G.; Chae, S.; Kim, G.; Jong, G.; Jon, Y. *Sci. Rep.* **2019**, *9* (1), 20264.
- [30]. Al-Sawaff, Z.; Sayiner, H. S.; Kandemirli, F. *J. Amasya Univ. Inst. Sci. Tech.* **2020**, *1* (1), 1–11.
- [31]. Shntaif, A. H.; Rashi, Z. M.; Al-Sawaff, Z. H.; Kandemirli, F. *Russ. J. Bioorganic Chem.* **2021**, *47* (3), 777–783.
- [32]. Hossain, M. A.; Hossain, M. R.; Hossain, M. K.; Khandaker, J. I.; Ahmed, F.; Ferdous, T.; Hossain, M. A. *Chem. Phys. Lett.* **2020**, *754* (137701), 137701.
- [33]. Li, J.; Lu, Y.; Ye, Q.; Cinke, M.; Han, J.; Meyyappan, M. *Nano Lett.* **2003**, *3* (7), 929–933.
- [34]. Wu, N.; Ji, X.; An, R.; Liu, C.; Lu, X. *AIChE J.* **2017**, *63* (10), 4595–4603.
- [35]. Matta, C. F.; Bader, R. F. W. *Proteins* **2003**, *52* (3), 360–399.
- [36]. Lu, T.; Chen, F. *J. Comput. Chem.* **2012**, *33* (5), 580–592.
- [37]. Shamim, S. U. D.; Hussain, T.; Hossain, M. R.; Hossain, M. K.; Ahmed, F.; Ferdous, T.; Hossain, M. A. *J. Mol. Model.* **2020**, *26* (6), 1–17. <https://doi.org/10.1007/s00894-020-04419-z>
- [38]. Rahman, H.; Hossain, M. R.; Ferdous, T. *J. Mol. Liq.* **2020**, *320* (114427), 114427.
- [39]. Rezaei-Sameti, M.; Abdoli, S. K. *J. Mol. Struct.* **2020**, *1205* (127593), 127593.
- [40]. Shahabi, M.; Raissi, H. *J. Biomol. Struct. Dyn.* **2018**, *36* (10), 2517–2529.



Copyright © 2021 by Authors. This work is published and licensed by Atlanta Publishing House LLC, Atlanta, GA, USA. The full terms of this license are available at <http://www.eurjchem.com/index.php/eurjchem/pages/view/terms> and incorporate the Creative Commons Attribution-Non Commercial (CC BY NC) (International, v4.0) License (<http://creativecommons.org/licenses/by-nc/4.0>). By accessing the work, you hereby accept the Terms. This is an open access article distributed under the terms and conditions of the CC BY NC License, which permits unrestricted non-commercial use, distribution, and reproduction in any medium, provided the original work is properly cited without any further permission from Atlanta Publishing House LLC (European Journal of Chemistry). No use, distribution or reproduction is permitted which does not comply with these terms. Permissions for commercial use of this work beyond the scope of the License (<http://www.eurjchem.com/index.php/eurjchem/pages/view/terms>) are administered by Atlanta Publishing House LLC (European Journal of Chemistry).